Combinatorial Chemistry & High Throughput Screening, 2013, *16*, 000-000

Quantitative Structure-Activity Relationships of the Antimalarial Agent Artemisinin and Some of its Derivatives – A DFT Approach

Sanchaita Rajkhowa[1], Iftikar Hussain[1], Kalyan K. Hazarika[2], Pubalee Sarmah and Ramesh Chandra Deka[*,1]

[1]*Department of Chemical Sciences,* [2]*Department of Molecular Biology & Biotechnology, Tezpur University, Napaam, Tezpur - 784028, Assam, India*

Abstract: Artemisinin form the most important class of antimalarial agents currently available, and is a unique sesquiterpene peroxide occurring as a constituent of *Artemisia annua*. Artemisinin is effectively used in the treatment of drug-resistant *Plasmodium falciparum* and because of its rapid clearance of cerebral malaria, many clinically useful semisynthetic drugs for severe and complicated malaria have been developed. However, one of the major disadvantages of using artemisinins is their poor solubility either in oil or water and therefore, in order to overcome this difficulty many derivatives of artemisinin were prepared. A comparative study on the chemical reactivity of artemisinin and some of its derivatives is performed using density functional theory (DFT) calculations. DFT based global and local reactivity descriptors, such as hardness, chemical potential, electrophilicity index, Fukui function, and local philicity calculated at the optimized geometries are used to investigate the usefulness of these descriptors for understanding the reactive nature and reactive sites of the molecules. Multiple regression analysis is applied to build up a quantitative structure-activity relationship (QSAR) model based on the DFT based descriptors against the chloroquine-resistant, mefloquine-sensitive *Plasmodium falciparum* W-2 clone.

Keywords: Artemisinin, DFT, Electrophilicity index (ω), Fukui function (FF), Hardness (η), QSAR.

1. INTRODUCTION

Malaria remains one of the world's greatest public health challenges. Half of world's population is at the risk of malaria. Nearly a million deaths out of 247 million clinical episodes, mostly of children below 5 years of age were reported in the year 2006 [1]. In 2008, 109 countries were recognised as endemic for malaria with 3.3 billion people at risk among which 45 countries were within the WHO African region.

Plasmodium falciparum was among the leading causes of death worldwide in 2004 from a single infectious agent [2]. There are four members of the *Plasmodium* genus that infect humans *via* transmission through the bite of Anopheles female mosquito [3]. The parasite responsible for the majority of fatal malaria infections, *P. falciparum*, can kill patients in a matter of hours. Most of the strains of *P. falciparum* have now become resistant to chloroquine and other traditional antimalarials [4, 5]. However, artemisinin [6] (Fig. **1**), isolated from a Chinese medicinal herb is still found to be a potent antimalarial drug against the resistant strains of *P. falciparum*. Artemisinin as well as some of its derivatives are the most potent and rapidly acting antimalarial drugs at hand nowadays [7]. However, total synthesis and biochemical synthesis of artemisinin are not viable as the mainstream sources of artemisinin because these routes are not cost effective. Notwithstanding serious efforts, a successful malaria vaccine has remained a distant dream and therefore development of new antimalarials based on artemisinin is crucial to control and manage the disease.

The effectiveness of artemisinin and its derivatives as antimalarial drugs for the treatment of multi-drug-resistant *P. falciparum* has received considerable attention in recent years [8]. The development of a new drug is a very long and expensive process. It is thus ideal to have a method that enables a prediction of biological activity of new compounds in advance based on the knowledge of chemical structure alone. For drug discovery and development, quantitative structure–activity relationships (QSAR) technique [9] are often employed because the bioactivity of new compounds can be predicted effectively with reduced efforts. Traditional QSAR [10] studies have been used since the early 1970s to predict activities of untested molecules. Development of a QSAR based pharmacophore model [11] may be of great help to discover a pharmaceutically acceptable and economically viable peroxide-based antimalarial. QSAR studies were performed to correlate the biological activity/property of a series of compounds with some appropriate descriptors. Among different descriptors for describing the electronic properties of molecules, the quantum chemical descriptors based on DFT and semi-empirical methods have been found useful in several QSAR studies [12, 13]. In particular, net atomic charges, HOMO–LUMO energies, frontier orbital electron densities, and superdelocalizabilities have shown to correlate with various biological activities [14].

The performance of the DFT [15] method in the description of structural, energetic, and magnetic molecular properties has been quite substantially reviewed in recent

*Address correspondence to this author at the Department of Chemical Sciences, Tezpur University, Napaam, Tezpur - 784028, Assam, India; Tel: 91 3712 267008; Fax: 91 3712 267005; E-mail: ramesh@tezu.ernet.in

1386-2073/13 $58.00+.00

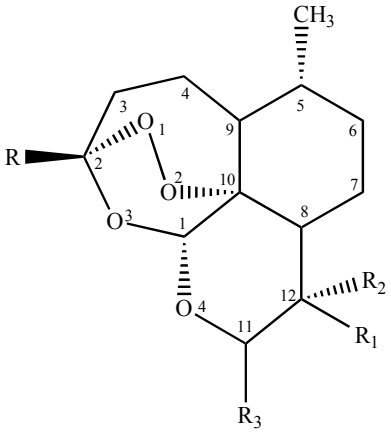

Molecule	R	R1	R2	R3	Log RA
1	CH_3	CH_3	H	.=O	0
2	CH_3	CH_3	H	OEt	0.34
3	CH_3	CH_3	H	OMe	0.28
4	CH_3	CH_3	H	OH	0.55
5	CH_3	H	CH_3	.=O	-0.17
6	CH_3	C_2H_5	H	.=O	1.4
7	C_4H_9	H	H	.=O	-0.74
8	C_2H_5	H	H	.=O	0.05
9	H	H	H	.=O	-2.76
10	C_3H_7	H	H	.=O	0.83
11	CH_3	.=CH_2	---	.=O	-0.89
12	CH_3	.=$CHCH_3$	---	.=O	-0.36
13	CH_3	.=O	---	.=O	-2.47
14	CH_3	C_5H_{11}	H	.=O	1.02
15	CH_3	C_3H_7	H	.=O	1.13
16	CH_3	CH_3	H	H	0.75
17	CH_3	CH_3	H	OH	0.55
18	CH_3	CH_3	H	OEt	0.34
19	CH_3	C_4H_9	H	OH	0.96
20	CH_3	H	H	H	0.28
21	CH_3	CH_3	H	OMe	0.28
22	CH_3	C_4H_9	H	H	1.32
23	CH_3	C_2H_5	H	H	0.67
24	CH_3	C_3H_7	H	OEt	0.04
25	CH_3	H	H	OEt	0.43
26	CH_3	C_2H_5	H	OEt	0.5
27	CH_3	CH_3	H	C_4H_9	0.06
28	CH_3	CH_3	H	OCH_2CO_2Et	0.52
29	$C_2H_4CO_2Et$	H	H	H	0.7
30	C_2H_5	H	H	H	-0.1
31	C_3H_7	H	H	H	0.84
32	CH_3	=CH_2		H	-2.39
33	CH_3	C_5H_{11}	H	H	0.16
34	CH_3	C_3H_7	H	H	0.74
35	CH_3	CH_3	OH	OEt	-0.44
36	CH_3	OH	CH_3	OEt	-1.13
37	CH_3	CH_3	Br	NH-2-(1,3-thiazole)	0.66
38	CH_3	CH_3	H	C_4H_9	0.06
39	CH_3	CH_3	H	OCH_2-adamantyl	0.28
40	CH_3	CH_3	H	OCH_2(*p*-$PhCO_2Me$)	-0.07

Fig. (1). Structures of artemisinin and its 39 analogues involved in this testing set using their relative activity.

times. DFT based reactivity descriptors namely, global hardness (η), electronegativity (χ), chemical potential (μ), electrophilicity index (ω), Fukui functions ($f(r)$) and philicity (ω_k^α), [16-20] have attracted considerable interests to describe reactivity and site selectivity of various bio-molecules [21, 22]. The electrophilicity and philicity indices have also been successfully used to predict the biological activity/toxicity/property of different organic molecules [23-25].

In this study we used DFT based reactivity descriptors to study the structure, stability, and reactivity of artemisinin and some of its derivatives. Theoretically obtained values are compared with experimental data. Experimentally proposed mechanism of action of artemisinin has been established theoretically by verifying that O1 of the endoperoxide linkage of artemisinin is the preferred site of electrophilic attack by the heme iron. DFT based global reactivity descriptors global softness and global electrophilicity, calculated at the optimized geometries are used to investigate the reactive nature of the molecules while local reactivity descriptors such as Fukui function and philicity are utilized for selecting the reactive site(s) in individual molecule. Multiple regression analyses were performed to build up a QSAR model based on DFT derived descriptors as well as molecular mechanics (MM) parameters for artemisinin to establish the importance of the descriptor in predicting antimalarial activity. The comparative QSAR study with the help of DFT techniques were performed in gas media and the training set correlation coefficients and cross-validation using test set values were found to be significant.

The mode of action of artemisinin derivatives is different from other antimalarial drugs because of their unusual structures. Artemisinin is a sesquiterpene lactone with an endoperoxide group, and its unusual 1,2,4-trioxane ring system has been proven to be critical for the antimalarial activity [26]. Although the precise mechanism of action of artemisinin is still very controversial [27]; the endoperoxide pharmacophore alone has led to the development of several different classes of totally synthetic endoperoxides including the trioxolanes OZ277 [28] and OZ439 [29] which are now in different phases of clinical trials. It is ensured that the selected analogues act *via* similar mechanisms of action. Biological activity have been taken from reported control activity for artemisinin where the selected compounds have been tested using the same assay method, i.e., *in vitro* against the chloroquine-resistant, mefloquine-sensitive *P. falciparum* W-2 clone [30, 31]. The relative activity (RA) for quantitative comparisons was calculated from the experimentally derived control IC_{50} of artemisinin (IC_{50} values in ng/mL) divided by the IC_{50} of the analogue and corrected for molecular weight. Before inclusion into the spreadsheets, the RA was converted to the log RA.

log RA= log[(IC50 of artemisinin/IC50 of the analog) × (MW of the analog/MW of artemisinin)]

2. METHODS

2.1. Theoretical Background

DFT provides a framework to calculate these descriptors in terms of changing number of electrons (N) or changing

external potential, $v(r)$ due to nuclei. The first derivatives of $E(\rho)$ with respect to the number of electron *N* under the constant external potential $v(r)$ is defined as the chemical potential μ that equals minus the electronegativity (χ).

$$\mu = \left(\frac{\delta E}{\delta N}\right)_{v(r)} = -\chi \quad (1)$$

Chemical hardness (η) of an electronic system is defined as the second derivative of energy (E) with respect to the number of electrons (N) at constant external potential, $v(r)$ [32].

$$\eta = \frac{1}{2}\left(\frac{\delta^2 E}{\delta N^2}\right)_{v(r)} = \frac{1}{2}\left(\frac{\delta \mu}{\delta N}\right)_{v(\bar{r})} \quad (2)$$

Using a finite difference method the working equations for calculation of chemical potential and chemical hardness can be approximated as

$$\mu = \frac{IP + EA}{2}, \quad \eta = \frac{IP - EA}{2} \quad (3)$$

where IP and EA are the first vertical ionization potential and the electron affinity, respectively, of the chemical system.

Further approximation using Koopmans' theorem [33] the above parameters can be expressed by taking IP and EA as negative of the HOMO and LUMO energies, respectively:

$$\mu = \frac{E_{LUMO} + E_{HOMO}}{2} \qquad \eta = \frac{E_{LUMO} - E_{HOMO}}{2} \quad (4)$$

where E_{HOMO} and E_{LUMO} are the energies of the highest occupied and lowest unoccupied molecular orbitals, respectively.

Parr *et al*. [34] proposed electrophilicity index as a measure of energy lowering due to maximal electron flow between donor and acceptor. They defined electrophilicity index (ω) as

$$\omega = \frac{\mu^2}{2\eta} = \frac{\chi^2}{2\eta} \quad (5)$$

When two molecules react with each other, one molecule behaves as an electrophile while the other acts as a nucleophile. Higher (lower) electrophilicity index indicates higher electrophilic (nucleophilic) character of a molecule.

The condensed Fukui functions [35] (FF) are calculated as follows:

$$f_k^+ = \frac{1}{\Delta N}[q_k(N_0 + \Delta N) - q_k(N_0)] \quad \text{(for nucleophilic attack)} \quad (6)$$

$$f_k^- = \frac{1}{\Delta N}[q_k(N_0) - q_k(N_0 - \Delta N)] \quad \text{(for electrophilic attack)} \quad (7)$$

where q_k is the electronic population of atom *k* in a molecule. In conventional FF computations, a value of 1.0 is used for ΔN . In the present calculation, we have used a value of 0.1 for ΔN .

Chattaraj *et al* [36] proposed local philicity as

$$\omega_k^\alpha = \omega f_k^\alpha \quad (8)$$

where f_k^α is the FF associated with α= +, -, and 0 referring to nucleophilic, electrophilic, and radical reactions, respectively.

Roy *et al*. [37] introduced two different local reactivity descriptors, "relative electrophilicity" $\left(f_k^+ / f_k^-\right)$ and "relative nucleophilicity" $\left(f_k^- / f_k^+\right)$ of any particular atom *k*, to locate the preferable site for nucleophilic and electrophilic attack on it, respectively. These two reactivity descriptors generate improved intramolecular as well as intermolecular reactivity trends than those obtained from condensed FF.

2.2. Computational Details

The artemisinin structure determined by X-ray crystallography [38] was considered as the most reliable reference structure and so was used as the basic structure. Full unconstrained geometry optimizations of artemisinin was carried out at gradient corrected DFT using the DMol^3 program. We used double numerical with polarization (DNP) basis set [39] in combination with several LDA and GGA exchange-correlation functionals like BLYP, BOP, HCTH, BP, PW91, PWC and VWN-BP.

Artemisinin and its 39 analogues (Fig. **1**) were optimized with most widely used exchange-correlation functional BLYP in combination with DNP basis set. The size of this DNP basis set is comparable to the 6-31G** basis of Hehre *et al*. [40]. However, they are believed to be much more accurate than a Gaussian basis set of the same size [41]. All molecules were characterized as minima (no imaginary frequency) in their potential energy surface through harmonic frequency analysis.

The global reactivity descriptors, such as chemical potential, μ chemical hardness, η and electrophilicity, ω have been calculated by using equations 4 and 5. FF were calculated using both Mulliken [42] (MPA) and Hirshfeld [43] population analysis (HPA). The molar refractivity parameter of carrier ligands and surface area of each complex were obtained from the MM+ computations with Hyperchem software [44].

2.3. QSAR Modeling

The logarithmic relative activity values (logRA) of compounds (1–40) were taken from the reference [30]. From the results of DFT calculations, various descriptors, such as energy of highest occupied molecular orbital (E_{HOMO}), energy of lowest unoccupied molecular orbital (E_{LUMO}), energy of the next lowest unoccupied molecular orbital (E_{NL}), energy difference between LUMO and HOMO ($\Delta_{L\text{-}H}$), dipole moments, electrophilicity (ω), hardness (η), philicity (ω^+) etc were selected for QSAR modelling. In addition, the molecular mechanics parameters such as molar refractivity (*MR*), van der Waals surface area (*SA*), molecular volume, log of octanol/water partition coefficient (*logP*) of the whole molecule and molar refractivities (MR_R, MR_{R1}, MR_{R2}, MR_{R3})

of the substituents (R, R_1, R_2, R_3) were selected. The descriptors with greater correlation to log RA with smaller autocorrelation were selected out to perform the stepwise multiple linear regression. The predictive power of the models was validated by the test set values.

3. RESULTS AND DISCUSSION

3.1. Geometry of Artemisinin

Complete geometry optimization of artemisinin was performed using DMol[3] program. The structures obtained using DNP basis set in combination with several functional such as HCTH, BLYP, PW91, PWC, BOP, BP, VWN-BP were compared with the available X-ray crystallography structure. Table **1** shows the experimental and calculated geometric parameters of artemisinin 1,2,4-trioxane ring. It can be seen from Table **1** that the bond lengths are well described by all calculations performed. Also, all calculated bond angles are nearly close to the available experimental values. The torsion angles of the twist boat conformation in artemisinin shows very good agreement between this work and the experimental values (47.4 degree). Since no significant variation of bond lengths and bond angles from the experimental data have been noticed with DNP basis set and any of the functional, the most popular exchange-correlation functional BLYP in combination with DNP basis set has been chosen for performing calculations for the remaining molecules.

Table 1. A Comparison of the Geometry of Artemisinin Optimized at Different Theoretical Levels with Experimental Results. Bond Lengths are in Å, Bond Angles and Dihedral Angles are in Degree

Geometry	Experimental	HCTH	BLYP	PW91	PWC	BOP	BP	VWN-BP
Bond Length								
C2C1	1.528	1.54	1.55	1.55	1.53	1.56	1.55	1.54
C3C2	1.559	1.53	1.55	1.54	1.52	1.55	1.54	1.54
C4C3	1.556	1.54	1.56	1.55	1.52	1.56	1.55	1.55
C5C4	1.521	1.56	1.57	1.56	1.53	1.57	1.56	1.56
C5O6	1.456	1.45	1.48	1.46	1.43	1.48	1.46	1.46
O6O7	1.478	1.46	1.51	1.49	1.45	1.51	1.49	1.49
O7C1	1.403	1.41	1.42	1.42	1.40	1.43	1.42	1.41
C1O8	1.437	1.45	1.47	1.46	1.43	1.47	1.46	1.46
O8C9	1.390	1.39	1.41	1.40	1.38	1.41	1.40	1.40
C9C5	1.529	1.53	1.54	1.54	1.52	1.55	1.54	1.54
Bond Angle								
O6O7C1	107.5	108.4	107.7	107.8	107.7	107.9	107.8	107.7
O7C1O8	107.3	108.6	108.4	108.6	108.4	108.5	108.6	108.6
C1O8C9	114.1	113.8	114.0	113.8	113.0	114.0	113.4	113.4
O8C9C5	113.3	113.5	113.9	113.8	113.3	114.0	113.8	113.9
C9C5O6	111.0	111.4	111.7	111.8	111.8	111.6	111.8	111.8
C5O6O7	111.1	111.7	111.3	111.2	110.7	111.4	111.2	111.1
C9C5C4	111.6	111.1	111.2	111.0	110.4	111.3	111.0	111.0
O6C5C4	106.2	105.9	116.7	105.9	106.6	105.6	105.9	105.8
C5C4C3	112.2	112.1	112.2	112.1	112.0	112.2	112.1	112.0
C4C3C2	115.1	116.5	116.7	116.6	116.2	116.8	116.6	116.7
C3C2C1	112.6	114.3	114.6	114.4	113.8	114.7	114.4	114.4
C2C1O7	112.3	111.9	112.2	112.3	111.9	112.2	112.3	112.3
C2C1O8	110.6	109.4	109.4	109.3	109.3	109.4	109.3	109.3
Dihedral Angle								
C5O6O7C1	47.4	47.1	46.9	47.4	49.5	46.5	47.4	47.8
O6O7C1O8		-73.7	-73.7	-74.2	-75.5	-73.4	-74.2	-74.4
O7C1O8C9		33.3	34.6	34.1	32.9	34.6	34.1	34.1
C1O8C9C5		26.9	26.5	26.8	28.0	26.4	26.8	26.9

3.2. Global Descriptors

Global reactivity parameters such as chemical potential (μ), hardness (η), electrophilicity index (ω) of artemisinin and all the 40 derivatives have been calculated at the BLYP/DNP level and they are presented in Table **2**.

According to maximum hardness principle (MHP) [45], at constant external potential, stability of a molecule increases with hardness and with the increase in stability the reactivity decreases. It is seen from Table **2** that the molecule 13 has the lowest chemical hardness (η) value (1.3705 eV) among the all modelled derivatives and hence is the most reactive one. The variation of hardness (η) calculated with BLYP/ DNP level for the molecules are shown in Fig. (**2a**).

On the other hand, electrophilicity index (ω) is considered as a measure of electrophilic power of a molecular system towards

Table 2. A Comparison of the Reactivity Descriptors of Artemisinin and Various Derivatives Optimized at BLYP/DNP Theoretical Levels in Gas Phase

Molecule	Chemical Potential (μ)	Hardness (η)	Electrophilicity (ω)
1	-3.962	1.972	3.980
2	-3.485	1.893	3.208
3	-3.509	1.884	3.268
4	-3.547	1.914	3.311
5	-3.969	1.944	4.052
6	-3.970	1.945	4.052
7	-3.978	1.952	4.053
8	-3.976	1.957	4.039
9	-4.114	1.909	4.433
10	-3.985	1.945	4.082
11	-4.097	1.836	4.571
12	-3.967	1.879	4.188
13	-4.573	1.371	7.628
14	-3.948	1.955	3.986
15	-3.955	1.955	4.211
16	-3.468	1.874	3.209
17	-3.573	1.894	3.370
18	-3.495	1.879	3.250
19	-3.611	1.891	3.448
20	-3.486	1.868	3.253
21	-3.510	1.885	3.268
22	-3.456	1.869	3.195
23	-3.477	1.853	3.262
24	-3.488	1.876	3.243
25	-3.502	1.882	3.258
26	-3.482	1.882	3.221
27	-3.411	1.859	3.129
28	-3.688	1.914	3.553
29	-3.624	1.881	3.491
30	-3.461	1.874	3.196
31	-3.457	1.875	3.187
32	-3.567	1.889	3.368
33	-3.448	1.874	3.172
34	-3.456	1.869	3.195
35	-3.717	1.723	4.009
36	-3.575	1.884	3.392
37	-3.860	1.284	5.803
38	-3.592	1.736	3.716
39	-3.658	1.743	3.838
40	-3.974	1.461	5.405

Chemical potential (μ in eV), hardness (η in eV) and electrophilicity index (ω in eV) values calculated from orbital consideration are presented.

a nucleophile. Larger the electrophilic power of a chemical system, higher is its reactivity as an electrophile. Conversely, lower is the electrophilic power of a chemical system higher is its reactivity as a nucleophile. The variation of electrophilicity index (ω) calculated with BLYP/ DNP level for the molecules is shown in Fig. (**2b**). It can be seen from Fig. (**2b**) that molecule 13 has maximum electrophilicity value which is comparable to molecules 40, 9 and 11. Thus from ω values the molecules 9, 11, 13 and 40 are found to be more reactive than the other compounds.

However, other global descriptor, chemical potential is observed to be less significant to predict any reactivity trend of the molecules correctly. Hence, there is a need for more reliable parameter to describe reactivity of these molecules.

3.3. Local Descriptors

Local reactivity parameters such as fukui function (FF) describe the relative reactivity and site selectivity of atoms in a molecule. The nucleophilic attack at a particular site of a system represents the sites with maximum values of FF, (f_k^+) and/or local philicity, ω_k^+. Similarly, electrophilic attack at a particular site of a system represents the sites with maximum values of FF, f_k^- and/or local philicity, ω_k^-.

We calculated FF for all the atoms in artemisinin and its derivatives to derive the most reactive atoms in each of the molecules. From the FF values it was found that the atoms O1 and O2 are the most reactive atoms in each of the molecule. Therefore we considered FF, local philicity and relative nucleophilicity values of O1 and O2 atoms for comparison.

3.4. Fukui function, (f_k^-)

FF values (f_k^-) of O1 and O2 atoms of artemisinin and derivatives derived from MPA and HPA schemes using BLYP/DNP levels are listed in Table **3**. It is seen from Table **3** that in almost all the molecules the value of (f_k^-) is higher in case of atom O1 than that of atom O2. This indicates that atom O1 is the preferred site for electrophilic attack which establishes the preference of heme iron to approach the O1 atom at the endoperoxide linkage of artemisinin compounds. While the f_k^- values of atom O1 are compared for all the molecules it does not show any significant variation. Similarly, f_k^- values of atom O2 also does not show any significant variation. Therefore, from f_k^- values of O1 and O2 atoms, it is difficult to compare the reactivity of the molecules.

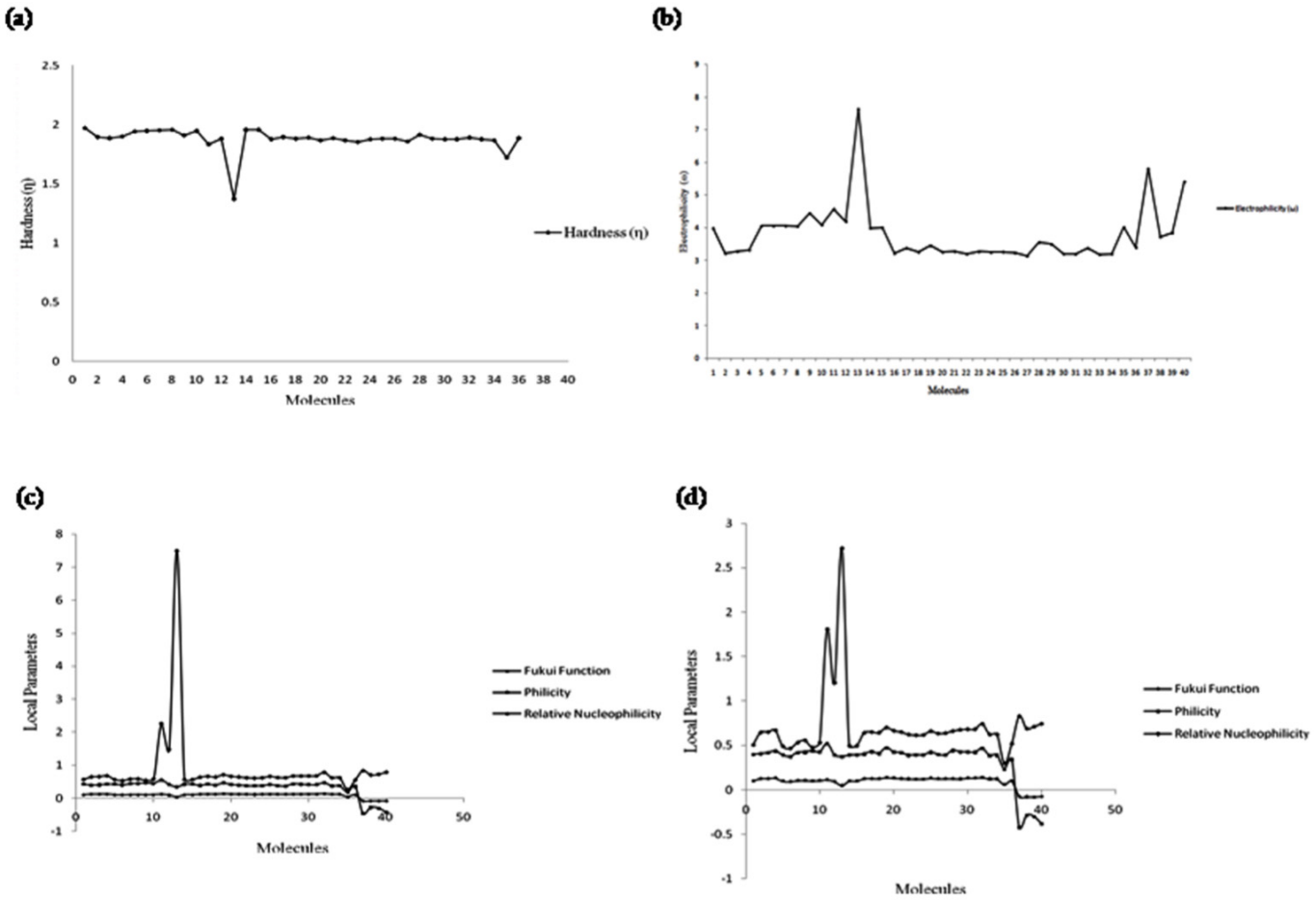

Fig. (2). Variation of global and local reactivity descriptors calculated at BLYP/DNP level: (**a**) hardness of the molecules, (**b**) electrophilicity of the molecules, (**c**) O1 atoms of all 40 artemisinin derivatives calculated at BLYP/DNP level using Hirshfeld Population Analysis, (**d**) O2 atoms of all 40 artemisinin derivatives calculated at BLYP/DNP level using Hirshfeld Population Analysis.

Table 3. Calculated Fukui Function (f_k^-), Local Philicity (ω_k^-) and Relative Nucleophilicity (f_k^-/f_k^+) Values for O1 and O2 Atoms of Artemisinin (Molecule 1) and Derivatives

Molecule	Mulliken						Hirshfeld					
	f_k^-		ω_k^-		f_k^-/f_k^+		f_k^-		ω_k^-		f_k^-/f_k^+	
	O1	O2	O1	O2	O1	O2	O1	O2	O1	O2	O1	O2
1	0.126	0.107	0.501	0.426	0.589	0.482	0.107	0.102	0.426	0.398	0.566	0.505
2	0.146	0.133	0.468	0.427	0.676	0.607	0.123	0.127	0.395	0.407	0.647	0.645
3	0.148	0.134	0.484	0.438	0.682	0.612	0.124	0.128	0.405	0.418	0.653	0.651
4	0.153	0.138	0.507	0.457	0.705	0.63	0.129	0.132	0.427	0.437	0.679	0.672
5	0.125	0.104	0.507	0.421	0.581	0.473	0.105	0.097	0.425	0.393	0.561	0.493
6	0.118	0.099	0.478	0.401	0.551	0.446	0.104	0.092	0.405	0.373	0.532	0.465
7	0.129	0.111	0.523	0.454	0.611	0.543	0.109	0.104	0.442	0.422	0.580	0.531
8	0.131	0.112	0.529	0.452	0.615	0.505	0.111	0.105	0.448	0.424	0.587	0.556
9	0.123	0.103	0.545	0.457	0.562	0.464	0.105	0.112	0.465	0.443	0.541	0.476
10	0.129	0.112	0.527	0.457	0.608	0.505	0.111	0.104	0.449	0.425	0.585	0.531
11	0.140	0.122	0.640	0.558	2.295	1.821	0.122	0.114	0.549	0.521	2.264	1.811
12	0.116	0.142	0.486	0.419	1.468	1.205	0.099	0.094	0.415	0.394	1.478	1.205
13	0.055	0.054	0.424	0.412	13.75	3.021	0.045	0.049	0.343	0.374	7.504	2.722
14	0.125	0.105	0.498	0.419	0.581	0.473	0.106	0.098	0.423	0.391	0.561	0.495
15	0.125	0.105	0.504	0.423	0.581	0.473	0.106	0.098	0.424	0.392	0.561	0.495
16	0.145	0.132	0.465	0.424	0.668	0.603	0.121	0.126	0.388	0.404	0.637	0.642
17	0.150	0.134	0.506	0.452	0.691	0.612	0.126	0.128	0.425	0.431	0.660	0.65
18	0.146	0.132	0.475	0.429	0.673	0.603	0.122	0.126	0.397	0.412	0.642	0.643
19	0.159	0.146	0.548	0.503	0.742	0.664	0.134	0.138	0.462	0.476	0.709	0.701
20	0.151	0.137	0.491	0.446	0.693	0.626	0.126	0.131	0.413	0.426	0.663	0.665
21	0.148	0.133	0.484	0.435	0.682	0.607	0.123	0.128	0.402	0.418	0.644	0.652
22	0.14	0.127	0.447	0.406	0.645	0.582	0.117	0.122	0.374	0.391	0.616	0.622
23	0.138	0.126	0.451	0.411	0.636	0.575	0.115	0.121	0.375	0.395	0.605	0.614
24	0.141	0.126	0.454	0.409	0.648	0.578	0.117	0.121	0.379	0.392	0.616	0.617
25	0.153	0.136	0.489	0.443	0.691	0.621	0.126	0.134	0.411	0.424	0.661	0.661
26	0.143	0.129	0.461	0.416	1.153	0.592	0.119	0.124	0.383	0.399	0.626	0.633
27	0.141	0.130	0.441	0.407	0.653	0.594	0.117	0.125	0.366	0.391	0.619	0.638
28	0.145	0.132	0.515	0.469	0.697	0.629	0.123	0.125	0.437	0.444	0.672	0.661
29	0.144	0.128	0.503	0.447	0.706	0.627	0.121	0.123	0.422	0.429	0.672	0.676
30	0.153	0.142	0.489	0.447	0.712	0.636	0.128	0.133	0.409	0.425	0.674	0.682
31	0.152	0.141	0.484	0.446	0.713	0.636	0.128	0.133	0.408	0.424	0.677	0.682
32	0.164	0.145	0.552	0.488	0.824	0.707	0.139	0.138	0.468	0.465	0.781	0.742
33	0.141	0.128	0.447	0.406	0.653	0.587	0.117	0.122	0.371	0.387	0.616	0.622
34	0.141	0.127	0.45	0.406	0.65	0.583	0.117	0.122	0.374	0.390	0.616	0.622
35	0.056	0.061	0.225	0.245	0.265	0.281	0.047	0.058	0.188	0.233	0.257	0.296
36	0.126	0.106	0.427	0.361	0.578	0.488	0.104	0.101	0.353	0.343	0.552	0.518
37	-0.272	0.275	-1.580	-1.596	0.938	0.942	-0.079	-0.073	-0.46	-0.422	0.833	0.829
38	-0.258	-0.26	-0.961	-0.966	0.881	0.867	-0.076	-0.077	-0.28	-0.285	0.703	0.689
39	-0.261	-0.263	-1.001	-1.009	0.891	0.877	-0.078	-0.078	-0.301	-0.301	0.723	0.711
40	-0.276	-0.259	-1.492	-1.421	0.923	0.866	-0.079	-0.071	-0.43	-0.381	0.788	0.743

These values are evaluated using BLYP/DNP level using HPA and MPA charges.

3.5. Local Philicity (ω_k^-)

Philicity is considered as better intermolecular reactivity parameter than FF for analyzing electrophile-nucleophile interactions as it is the product of global and local parameter. Philicity (ω_k^-) values O1 and O2 atoms of artemisinin and derivatives derived from MPA and HPA schemes using BLYP/DNP levels are listed in Table **3**. However, variation of philicity is also observed to be less significant to make a comparison among the molecules to predict their reactivity.

3.6. Relative Nucleophilicity, (f_k^- / f_k^+)

The relative nucleophilicity, (f_k^- / f_k^+) values of O1 and O2 atoms of artemisinin and derivatives derived from MPA and HPA schemes at BLYP/DNP level are reported in Table **3**. It is noticed from Table **3** that f_k^- / f_k^+ values of O1 atom thus calculated increase in the order: molecule 12 < molecule 11 < molecule 13. Therefore, molecule 13 shows maximum reactivity towards a nucleophile followed by molecules 11 and 12. The variation of relative nucleophilicity calculated with BLYP/ DNP level for the molecules are shown in Fig. (**2c**, **d**).

3.7. QSAR Studies

The logarithmic relative activity values (logRA) of compounds (1–40) were taken from the reference [30]. The analyses were performed in gas media. The QSAR equation having significant statistical parameters for 40 artemisinin analogues is represented by equation 10. The equation is obtained by considering the relative activity (logRA) as a dependent variable and electrophilicity (ω), energy of lowest unoccupied molecular orbital (E_{LUMO}), *logP*, and molar refractivity of R_3 group (MR_{R3}) as independent variables, values of which are presented in Table **4**.

$$LogRA = 2.689 + 0.702\omega(\pm 1.068) + 3.451E_{LUMO}(\pm 2.796) + 0.315LogP(\pm 0.156) - 0.024MR_{R3}(\pm 0.027) \quad (10)$$

n = 40, r^2 = 0.291, SD = 0.838, F = 3.585, p<0.05

Here, r^2 is the square of correlation coefficient, *SD* is the standard deviations of regression, *F* is the overall *F*-statistics for the addition of each successive term, and *p* is the *p*-values using the *F*-statistics. In general, a regression model is significant at *p*-value < 0.05 using the *F* statistics [46] and so these models are statistically significant. However, according to the generally statistical standards, a model with r^2 > 0.80 [47] is acceptable. Therefore, these QSAR equations should be further improved to become a statistically significant model.

To improve r^2, LOO (Leave One Out) method suggested by Dietrich *et al*. [48] was applied in which a compound is considered as outlier if its corresponding r^2, called jackknife r^2 (r_j^2) value obtained from the regression analysis after deleting the compound, is comparatively higher than the other r_j^2 values. The calculated r_j^2 values are presented in Table **4**. It is clear from the table that compounds 6, 7, 10, 13, 24, 25, 27, 30, 32, 33, 37 and 40 have higher r_j^2 values. But the model that we have developed after deleting these compounds is not found to be significant. So, we have used various combinations of r_j^2 to find the best fit model with the experimental data. We have fixed certain r_j^2, having higher values, with that of the various other combinations of jackknife r^2 (r_j^2) values and found that removing 6, 7, 10, 24, 25, 27, 30, 32, 33, 35, 37 and 40 gave us a significant QSAR model, equation 11.

$$LogRA = 5.752 + 2.135\omega(\pm 0.571) + 8.915E_{LUMO}(\pm 1.554) + 0.729LogP(\pm 0.099) - 0.044MR_{R3}(\pm 0.016) \quad (11)$$

n = 28, r^2 = 0.867, SD = 0.377, F = 37.541, p<0.05

Equations 10 and 11 reveal that increasing values of ω, E_{LUMO} and *logP* and decreasing values MR_{R3} enhance the activity of artemisinin derivatives. Table **5** lists the experimental and calculated logRA values of the molecules. A plot between the experimental and calculated logRA values (Fig. **3**) shows that the selected descriptors are capable of predicting the activity of artemisinin derivatives.

3.8. Validation of the Developed Model

The predictive power of the developed model has been validated both internally (using Leave-One-Out cross validation) and externally (using training and test sets). Here the dataset were divided randomly into training set (75% of the total dataset) and test set (the remaining 25%) for external validation. The molecules **6**, **10**, **24**, **25**, **30**, **32**, **33**, **35**, **37** and **40** were selected as the test set and the remaining 30 molecules were treated as training set. The QSAR equation for the training set using the same descriptors were used to develop the model equation 12 as shown below.

$$LogRA = 5.842 + 2.053\omega(\pm 0.667) + 8.541E_{LUMO}(\pm 1.809) + 0.616Lo \quad (12)$$

n = 30, r^2 = 0.801, SD = 0.450, F = 25.203, p<0.05

Equations 12 showed similar statistical qualities as of equation 11. The results of the experimental and calculated values of the test set molecules (Table **6**) **6**, **10**, **24**, **25**, **30**, **32**, **33**, **35**, **37** and **40** showed similar calculated values in both the equations 11 and 12. This indicates significant predictive power of our developed model.

4. CONCLUSIONS

In this study we used DFT based reactivity descriptors to study the structure, stability, and reactivity of artemisinin and some of its derivatives. Comparison with experimental X-ray crystallographic structure data indicates that the optimized geometries of artemisinin obtained theoretically are in agreement with experimental values. From our study, it is clear that molecule 13 is found to be most reactive amongst the artemisinin derivatives based on the global hardness parameters. The electrophilicity value of molecule 13 is found to be maximum which is comparable with that of molecules 9 and 11. Fukui function (f_k^-) values of all the atoms of each of the molecule show that atom O1 is the most

Table 4. Parameters Used to Build the QSAR Models Along with the Jackknife Results for the Selected Set of Artemisinin Derivatives

Molecule	Electrophilicity (ω)	E_{LUMO}	Log P	MR_{R3}	LogRA	r_j^2
1	3.980	-1.991	4.71	1.95	0	0.291
2	3.208	-1.592	3.47	12.06	0.34	0.294
3	3.268	-1.625	3.13	7.32	0.28	0.293
4	3.311	-1.647	2.85	2.56	0.55	0.291
5	4.052	-2.025	4.71	1.95	-0.17	0.291
6	4.052	-2.025	5.11	1.95	1.4	**0.308**
7	4.053	-2.026	5.57	1.95	-0.74	**0.307**
8	4.039	-2.019	4.77	1.95	0.05	0.291
9	4.433	-2.205	3.59	1.95	-2.76	0.259
10	4.082	-2.04	5.17	1.95	0.83	**0.297**
11	4.571	-2.261	4.82	1.95	-0.89	0.276
12	4.188	-2.088	5.14	1.95	-0.36	0.291
13	7.628	-3.202	5.64	1.95	-2.47	0.343
14	3.986	-1.993	6.29	1.95	1.02	0.281
15	4.001	-2.021	5.5	1.95	1.13	0.291
16	3.209	-1.594	3.06	0.89	0.75	0.286
17	3.371	-1.679	2.85	2.56	0.55	0.293
18	3.252	-1.616	3.47	12.06	0.34	0.292
19	3.448	-1.722	4.04	2.56	0.96	0.285
20	3.253	-1.618	2.66	0.89	0.28	0.292
21	3.268	-1.625	3.13	7.32	0.28	0.293
22	3.195	-1.587	4.25	0.89	1.32	0.268
23	3.262	-1.624	3.46	0.89	0.67	0.285
24	3.243	-1.612	4.27	12.06	0.04	**0.295**
25	3.258	-1.620	2.97	12.06	0.43	**0.294**
26	3.221	-1.601	3.87	12.06	0.5	0.288
27	3.129	-1.552	4.73	19.46	0.06	**0.299**
28	3.553	-1.774	5.06	19.45	0.52	0.293
29	3.491	-1.743	4.64	0.89	0.7	0.284
30	3.196	-1.587	3.23	0.89	-0.1	**0.299**
31	3.187	-1.582	3.62	0.89	0.84	0.281
32	3.368	-1.678	2.97	2.56	-2.39	**0.372**
33	3.172	-1.574	4.64	0.89	0.16	**0.314**
34	3.195	-1.587	3.85	0.89	0.74	0.282
35	4.009	-1.994	2.53	12.06	-0.44	**0.292**
36	3.392	-1.691	2.53	12.06	-1.13	0.28
37	5.803	-2.576	3.44	2.5	0.66	**0.403**
38	3.716	-1.856	4.73	2.91	0.06	0.292
39	3.838	-1.915	5.52	1.62	0.28	0.291
40	5.405	-2.513	3.53	1.62	-0.07	**0.339**

Table 5. Experimental and Calculated logRA Values of Artemisinin and Derivatives from BLYP/DNP Level

Molecule	logRA		
	Experimental[a]	Calculated	Residual[b]
1	0	-0.14	0.14
2	0.34	0.41	-0.07
3	0.28	0.2	0.08
4	0.55	0.1	0.45
5	-0.17	-0.3	0.13
6	1.4	-0.01	1.41
7	-0.74	0.32	-1.06
8	0.05	-0.23	0.28
9	-2.76	-1.91	-0.85
10	0.83	-0.04	0.87
11	-0.89	-1.22	0.33
12	-0.36	-0.26	-0.1
13	-2.47	-2.48	0.01
14	1.02	0.99	0.03
15	1.13	0.39	0.74
16	0.75	0.58	0.17
17	0.55	-0.06	0.61
18	0.34	0.28	0.06
19	0.96	0.61	0.35
20	0.28	0.17	0.11
21	0.28	0.2	0.08
22	1.32	1.48	-0.16
23	0.67	0.72	-0.05
24	0.04	0.89	-0.85
25	0.43	-0.1	0.53
26	0.5	0.65	-0.15
27	0.06	1.19	-1.13
28	0.52	0.36	0.16
29	0.7	1.01	-0.13
30	-0.1	0.74	-0.84
31	0.84	1.05	-0.21
32	-2.39	0.04	-2.43
33	0.16	1.83	-1.67
34	0.74	1.19	-0.45
35	-0.44	-2.15	1.71
36	-1.13	-0.77	-0.36
37	0.66	-2.43	3.09
38	0.06	0.46	-0.4
39	0.28	0.83	-0.55
40	-0.07	-2.61	2.54

[a]From reference [30]. [b]Difference between the experimental and calculated values of logRA.

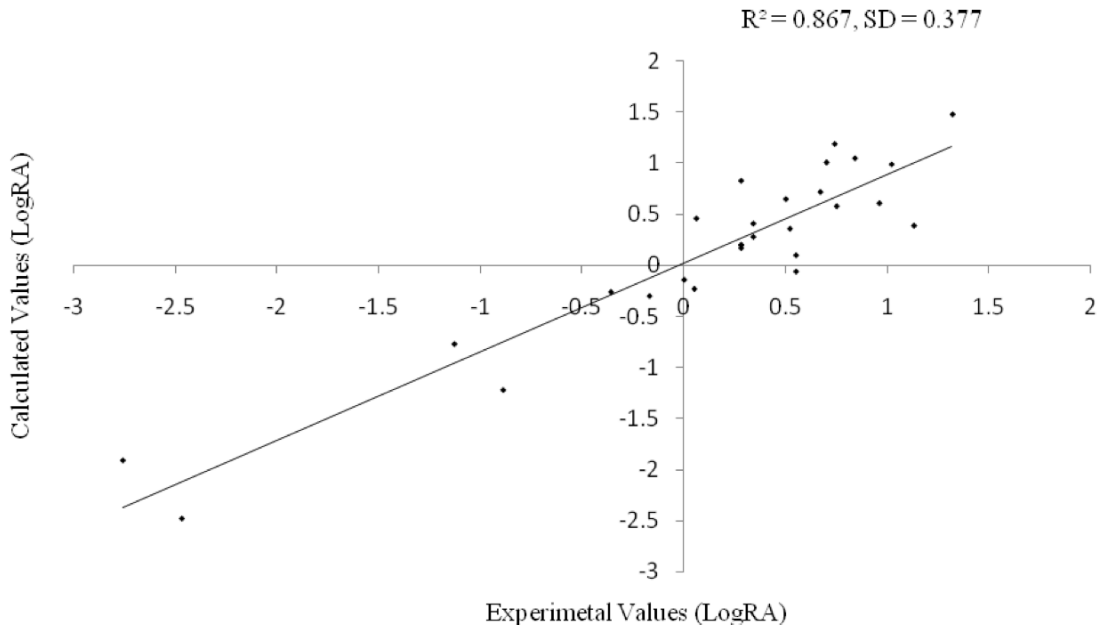

Fig. (3). A plot between experimental and calculated logRA values of all artemisinin derivatives.

Table 6. Experimental and Calculated logRA Values of Test Set Molecules Using Equation 12 (Training Set)

Molecules	logRA (Equation 11)			logRA (Equation 12)		
	Experimental[a]	Calculated	Residual[b]	Experimental[a]	Calculated	Residual[b]
6	1.4	-0.01	1.41	1.4	-0.1	1.5
10	0.83	-0.04	0.87	0.83	-0.13	0.96
24	0.04	0.89	-0.85	0.04	0.65	-0.61
25	0.43	-0.1	0.53	0.43	-0.19	0.62
30	-0.1	0.74	-0.84	-0.1	0.79	-0.89
32	-2.39	0.04	-2.43	-2.39	0.1	-2.49
33	0.16	1.83	-1.67	0.16	1.72	-1.56
35	-0.44	-2.15	1.71	-0.44	-2.11	1.67
37	0.66	-2.43	3.09	0.66	-2.27	2.93
40	-0.07	-2.61	2.54	-0.07	-2.45	2.38

[a]From reference [27]. [b]Difference between the experimental and calculated values of logRA.

reactive atom compared to other atoms. This also indicates that atom O1 is the preferred site for electrophilic attack which reveals that heme iron prefers to approach the O1 atom at the endoperoxide linkage of artemisinin compounds in agreement with the experimentally proposed mechanism of action of artemisinin compounds. The relative nucleophilicity, (f_k^- / f_k^+) shows that compound 13 has maximum reactivity followed by compounds 11 and 12. In summary, the comparative QSAR study with the help of DFT and MM + techniques provide the importance of the selected descriptors in predicting activity of the artemisinin analogues and provide important information about the structural requirements for the design of anti-malarial drugs.

CONFLICT OF INTEREST

The authors confirm that this article content has no conflicts of interest.

ACKNOWLEDGEMENTS

The authors are thankful to the Department of Science and Technology (DST) New Delhi for financial support.

REFERENCES

[1] World Health Organisation. Programmes and Projects: World Malaria Report 2008. http://www.who.int/malaria/wmr2008 (Accessed March 22, 2012).

[2] World Health Organisation. Programmes and Projects: Global burden of disease: 2004 update (2008). www.who.int/healthinfo/bodestimates/en/index.html (Accessed March 24, 2012).

[3] Pinheiro, J. C.; Kiralj, R.; Ferreira, M. M. C.; Romero, O. A. S. Artemisinin Derivatives with Antimalarial Activity against Plasmodium falciparum Designed with the Aid of Quantum Chemical and Partial Least Squares Methods. *QSAR Comb. Sci.*, **2003**, *22*(8), 830-842.

[4] O'Neill, P. M.; Posner, G. H.; A Medicinal Chemistry Perspective on Artemisinin and Related Endoperoxides. *J. Med. Chem.,* **2004**, *47*(12), 2945-2964.

[5] Posner, G. H.; O'Neill, P. M. Knowledge of the Proposed Chemical Mechanism of Action and Cytochrome P450 Metabolism of Antimalarial Trioxanes Like Artemisinin Allows Rational Design of New Antimalarial Peroxides. *Acc. Chem. Res.,* **2004**, *37*(6), 397-404.

[6] Klayman, D. L. Qinghaosu (artemisinin): an antimalarial drug from China. Science, **1985**, *228*, 1049-1055.

[7] Haynes, R. K.; Ho, W. Y.; Chan, H. W.; Fugmann, B.; Stetter, J.; Croft, S. L.; Vivas, L.; Peters, W.; Robinson, B. L. Highly Antimalaria-Active Artemisinin Derivatives: Biological Activity Does Not Correlate with Chemical Reactivity. *Angew. Chem. Int.,* **2004**, *43*(11), 1381-1385.

[8] Vroman, J. A. ; Alvim-Gaston, M. ; Avery, M. A. Current progress in the chemistry, medicinal chemistry and drug design of artemisinin based antimalarials. *Curr. Pharm. Des.,* **1999**, *5*, 101-138.

[9] Tonmunphean, S.; Parasuk, V.; Kokpol, S. QSAR Study of Antimalarial Activities and Artemisinin-Heme Binding Properties Obtained from Docking Calculations. *Quant. Struct. Act. Relat.,* **2000**, *19*(5), 475-483.

[10] Hansch, C.; Fujita, T. p-σ-π Analysis. A Method for the Correlation of Biological Activity and Chemical Structure. *J. Am. Chem. Soc.,* **1964**, *86*(8), 1616-1626.

[11] Avery, M. A.; McLean, G.; Edwards, G.; Ager, A. In: Biologically Active Natural Products: Pharmaceuticals; Stephen J. Cutler; Horace G. Cutler, Ed.; CRC Press, Boca Raton, Florida, **2000**; Vol. *8*, pp.121-132.

[12] Wan, J.; Zhang, L.; Yang, G. Quantitative structure–activity relationships for phenyl triazolinones of protoporphyrinogen oxidase inhibitors: A density functional theory study. *J. Comput. Chem.,* **2004**, *25*(15), 1827-1832.

[13] Srivastava, H. K.; Pasha, F. A.; Singh, P. P. Atomic softness-based QSAR study of testosterone. *Int. J. Quantum Chem.,* **2005**, *103*(3), 237-245.

[14] Karelson, M.; Lobanov, V. S. Quantum-Chemical Descriptors in QSAR/QSPR Studies. *Chem. Rev.,* **1996**, *96*(3), 1027-1044.

[15] Parr, R. G.; Yang, W. Density Functional Theory of Atoms and Molecules, Oxford University Press: New York, 1989

[16] Parr, R. G.; Pearson, R. G. Absolute hardness: companion parameter to absolute electronegativity. *J. Am. Chem. Soc.,* **1983**, *105*(26), 7512-7516.

[17] Parr, R. G.; Donnelly, R. A.; Levy, M.; Palke, W. E. Electronegativity: The density functional viewpoint. *J. Chem. Phys.,* **1978**, *68*(8), 3801-3807.

[18] Parr, R. G.; Szentpaly, L. V.; Liu, S. Electrophilicity Index. J. Am. Chem. Soc., **1999**, 121(9), 1922-1924.

[19] Parr, R. G.; Yang, W. Density functional approach to the frontier-electron theory of chemical reactivity. *J. Am. Chem. Soc.*, **1984**, *106*(14), 4049-4050.

[20] Chattaraj, P. K.; Maiti, B.; Sarkar, U. Philicity: A Unified Treatment of Chemical Reactivity and Selectivity. *J. Phys. Chem. A*, **2003**, *107*(25), 4973-4975.

[21] Chatterjee, A.; Balaji, T.; Matsunaga, H.; Mizukami, F. A reactivity index study to monitor the role of solvation on the interaction of the chromophores with amino-functional silanol surface for colorimetric sensors. *J. Mol. Graph. Model.*, **2006**, *25*(2), 208-218.

[22] Roos, G.; Loverix, S.; De Proft, F.; Wyns, L.; Geerlings, P. A Computational and Conceptual DFT Study of the Reactivity of Anionic Compounds: Implications for Enzymatic Catalysis. *J. Phys. Chem. A*, **2003**, *107*(35), 6828-6836.

[23] Parthasarathi, R.; Subramanian, V.; Roy, D. R.; Chattaraj, P. K. Electrophilicity index as a possible descriptor of biological activity. *Bioorg. Med. Chem.*, **2004**, *12*(21), 5533-5543.

[24] Padmanabhan, J.; Parthasarathi, R.; Subramanian, V.; Chattaraj, P. K. QSPR models for polychlorinated biphenyls: n-Octanol/water partition coefficient. *Bioorg. Med. Chem.,* **2006**, *14*(4), 1021-1028.

[25] Padmanabhan, J.; Parthasarathi, R.; Subramanian, V.; Chattaraj, P. K. Group Philicity and Electrophilicity as Possible Descriptors for Modeling Ecotoxicity Applied to Chlorophenols. *Chem. Res. Toxicol.,* **2006**, *19*(3), 356-364.

[26] Gu, J.; Chen, K.; Jiang, H.; Leszczynski, J. The Radical Transformation in Artemisinin: A DFT Study. *J. Phys. Chem. A*, **1999**, *103*(46), 9364-9369.

[27] Posner, G. W.; O' Neill, P. M. Knowledge of the proposed chemical mechanism of action and cytochrome p450 metabolism of antimalarial trioxanes like artemisinin allows rational design of new antimalarial peroxides. *Acc. Chem. Res.,* **2004**, *37*, 397-404.

[28] Vennerstrom, J. L.; Arbe-Barnes, S.; Brun, R.; Charman, S. A.; Chiu, F. C. K.; Chollet, J.; Dong, Y. X.; Dorn, A.; Hunziker, D.; Matile, H.; McIntosh, K.; Padmanilayam, M.; Tomas, J. S.; Scheurer, C.; Scorneaux, B.; Tang, Y. Q.; Urwyler, H.; Wittlin, S.; Charman, W. N. Identification of an antimalarial synthetic trioxolane drug development candidate. *Nature*, **2004**, *430*, 900-904.

[29] Charman, S. A.; Arbe-Barnes, S.; Bathurst, I. C.; Brun, R.; Campbell, M.; Charman, W. N.; Chiu, F. C. K.; Chollet, J.; Craft, J. C.; Creek, D. J.; Dong, Y.; Matile, H.; Maurer, M.; Morizzi, J.; Nguyen, T.; Papastogiannidis, P.; Scheurer, C.; Shackleford, D. M.; Sriraghavan, K.; Stingelin, L.; Tang, Y.; Urwyler, H.; Wang, X.; White, K. L.; Wittlin, S.; Zhou, L.; Vennerstrom, J. L. Synthetic ozonide drug candidate OZ439 offers new hope for a single-dose cure of uncomplicated malaria, Proceedings of the National Academy of Sciences, USA, February 7, 2011; Wellems, T. E.; National Institutes of Health, Bethesda, MD, **2011**, pp. 1-6.

[30] Avery, M. A.; Alvim-Gaston, M.; Rodrigues, C. R.; Barreiro, E. J.; Cohen, F. E.; Sabnis, Y. A.; Woolfrey, J. R. Structure−Activity Relationships of the Antimalarial Agent Artemisinin. 6. The Development of Predictive *In Vitro* Potency Models Using CoMFA and HQSAR Methodologies. *J. Med. Chem*., **2002**, *45*(2), 292-303.

[31] Milhous, W. K.; Weatherley, N. F.; Bowdre, J. H.; Desjardins, R. E. *In vitro* activities of and mechanisms of resistance to antifol antimalarial drugs. *Antimicrob. Agents Chemother.,* **1985**, *27*, 525-530.

[32] Parr, R. G.; Pearson, R. G. Absolute hardness: companion parameter to absolute electronegativity. *J. Am. Chem. Soc.,* **1983**, *105*(26), 7512-7516.

[33] Koopmans, T. A. Über die Zuordnung von Wellenfunktionen und Eigenwerten zu den Einzelnen Elektronen Eines Atoms. *Physica*, **1934**, *1*(1-6), 104-113.

[34] Parr, R. G.; Szentpaly, L. v.; Liu, S. Electrophilicity Index. J. Am. Chem. Soc., **1999**, *121*(9), 1922-1924.

[35] Fukui, K. Role of Frontier Orbitals in Chemical Reactions. *Science*, **1987**, *218*, 747-754.

[36] Chattaraj, P. K.; Maiti, B.; Sarkar, U. Philicity : A Unified Treatment of Chemical Reactivity and Selectivity. *J. Phys. Chem. A*, **2003**, *107*(25), 4973-4975.

[37] Roy, R. K.; Krishnamurti, S.; Geerlings, P.; Pal, S. Local Softness and Hardness Based Reactivity Descriptors for Predicting Intra- and Intermolecular Reactivity Sequences: Carbonyl Compounds. *J. Phys. Chem. A*, **1998**, *102* (21), 3746-3755.

[38] Lisgarten, J. N.; Potter, B. S.; Bantuzeko, C.; Palmer, R.A. Structure, absolute configuration, and conformation of the antimalarial compound, Artemisinin. *J. Chem. Cryst.,* **1998**, *28*(7), 539-543.

[39] Delley, B. An all-electron numerical method for solving the local density functional for polyatomic molecules. *J. Chem. Phys.,* **1990**, *92*, 508-517.

[40] Hehre, W. J. ; Radom, L.; Schleyer, P. V.; Pople, J. A. Ab Initio Molecular Orbital Theory; Wiley & Sons: New York, **1986**.

[41] Delley, B. From molecules to solids with the DMol3 approach. J. Chem. Phys., **2000**, *113*(18), 7756-7764.

[42] Mulliken, R. S. Electronic Population Analysis on LCAO☒MO Molecular Wave Functions. I. *J. Chem. Phys*., **1955**, *23*(10), 1833-1840.

[43] Hirshfeld, F. L. Bonded-atom fragments for describing molecular charge densities, *Theor. Chim. Acta.*, **1977**, *44*(2), 129-138.

[44] HyperChem; Release 7, Hypercube; http://www.hyper.com/, 2002.

[45] Pearson, R. G. Recent advances in the concept of hard and soft acids and bases. J. *Chem. Educ.*, **1987**, *64*(7), 561-567.

[46] Cho, D. H.; Lee, S. K.; Kim, B. T.; No, K. T. Quantitative Structure-Activity Relationship (QSAR) Study of New

Fluorovinyloxyacetamides. *Bull. Korean Chem. Soc.*, **2001**, *22*(4), 388-394.

[47] Yao, S. W.; Lopes, V. H. C.; Fernández, F.; García-Mera, X.; Morales, M.; Rodríguez-Borges, J. E.; Cordeiro, M. N. D. S. Synthesis and QSAR study of the anticancer activity of some novel indane carbocyclic nucleosides. *Bioorg. Med. Chem.*, **2003**, *11*(23), 4999-5006.

[48] Dietrich, S. W.; Dreyer, N. D.; Hansch, C.; Bentley, D. L. Confidence interval estimators for parameters associated with quantitative structure-activity relationships. *J. Med. Chem.*, **1980**, *23*(11), 1201-1205.

Received: August 2, 2012 **Revised: February 4, 2013** **Accepted: March 5, 2013**